GROUND TRUTH LOCATIONS USING SYNERGY BETWEEN REMOTE SENSING AND SEISMIC METHODS-APPLICATION TO CHINESE AND NORTH AFRICAN EARTHQUAKES

C. K. Saikia[1], H. K. Thio[2], D. V. Helmberger[2], G. Ichinose[1], and C. Ji[2]

URS Group, Inc.[1] and California Institute of Technology[2]

Sponsored by National Nuclear Security Administration
Office of Nonproliferation Research and Engineering
Office of Defense Nuclear Nonproliferation

Contract No. DE-AC52-03NA99505

ABSTRACT

The primary objective of this study is to establish ground truth (GT) locations of moderate to large magnitude earthquakes ($4.5<M_w<8$) occurring in China and North Africa using synergy between seismic and synthetic aperture radar interferometric methods. To this end, we have completed relocating earthquakes occurring in China and North Africa. In our last report, we have shown initial results from the Tibet (Manyi) earthquake (97/11/08, origin time 10h02m, latitude 35.069 E, longitude 87.325 N, preliminary determination of epicenters [PDE]; and $M_w = 7.5$) and its large aftershock (01/03/05, origin time 15h50m, latitude 34.369 N, longitude 86.902 E, and $M_w = 5.7$). We obtained the location of the mainshock by inverting surface deformation obtained by processing the satellite data and teleseismic waveforms together.

In this study, we have investigated the sensitivity of the method to location of the rupture initiation due to a variation in depth and along its strike direction. Our results show that for large earthquakes such as the Manyi mainshock, the waveforms remain insensitive, but the objective function that is used for the error analysis may still resolve the location. Using this new location, we estimated source-specific station corrections (SSSCs) for stations of the Chinese New Digital Station Network (CNDSN), using travel times obtained from the Chinese earthquake catalog. Using these SSSCs, we relocated many earthquakes occurring in its proximity for which we have travel times from the Chinese earthquake catalogs at common stations. Similar relocation was also done using travel times for earthquakes occurring in northeastern China (98/01/10, origin time 03h50m, latitude 41.11 N, longitude 114.55 E, and $M_w = 5.7$). We have also processed satellite data for several earthquakes that occurred in North Africa and ground deformation could be observed for two, one in Algeria (99/12/12, origin time 1h36m56.24s, latitude 35.32ºN, longitude 1.281ºW, h = 4.4 km, $M_w = 5.6$. National Earthquake Information Center [NEIC]) the other in Tunisia (97/03/20, origin time 18h02m17.98s, latitude 34.0046ºN, longiude 8.24ºE, h = 13.6 km, $M_w = 5.0$, International Seismological Centre [ISC]). Using both satellite and seismic data together, we established their new locations as follows: (a) Algerian event: latitude 34.963ºN and longitude 1.209ºW and (b) Tunisia event: latitude 34.0263ºN and longitude 8.288ºE. Using these relocations, we estimated SSSCs at stations that recorded these events and used the SSSCs at common stations to relocate many small earthquakes that occurred in their neighborhood.

OBJECTIVES

One of the most important problems in seismic monitoring is in determining GT locations so that the events can be used for calibration. Usually, large explosions provide the best GT location with error on the order of 1 km, but they are limited and one must rely primarily on earthquake data to extend the geographical coverage. Geodetic data, in the form of Synthetic Aperture Radar Interferometry (InSAR) measurements, provide much needed help in this process under some circumstances. The overall goal of this on-going study is to utilize geodetic data to establish high quality locations for shallow and moderate-sized earthquakes in Asia and North Africa in conjunction with seismic methods to validate GT location results. The work concentrates on events in North Africa (Algeria, Libya, Morocco, and Egypt), southwest Asia (Iraq and Iran, including China), and the Korean Peninsula. One of the major objectives of this study is to develop schemes to ascertain the location of rupture initiation on a given fault associated with large earthquakes. In this presentation, we will discuss earthquakes occurring in China, which have potential to become candidates for such GT events.

RESEARCH ACCOMPLISHED

November 8, 1997 (M_w 7.6) Tibet (Manyi) Mainshock

Our initial thrust here is in development of schemes that integrate both seismic and satellite data to establish the GT locations of large earthquakes. Earthquakes of magnitude greater than 6 at shallow depths provide strong co-seismic deformation that is easily discernable in satellite data, but unfortunately are difficult for establishing their epicenters. As pointed out in our previous report (Saikia et al., 2004), co-seismic deformation can be inverted for a dislocation fault model and the seismic data can then be inverted for a dislocation fault model and used to establish the time delays of these slip elements on the fault.

In our last report, we demonstrated the resolving power of InSAR in conjunction with seismic data for the November 8, 1997, M_w 7.6 Mayni (Tibetan) earthquake. This event occurred along the Kunlun fault as shown in Figure 1. The fault that ruptured has been studied by Tapponier and Molnar (1977) and a portion of it ruptured earlier in 1973. Three epicenters for the main event were reported; two based on the teleseismic data (centroid moment tensor, United States Geological Survey [USGS]) and one based on the regional travel time data as published by the Chinese Seismological Bureau, Beijing. The fault breakage outlined in Figure 1 is discussed in Peltzer et al. (1999).

We used a waveform inversion procedure developed by Ji et al. (2002a, b), which uses wavelet transforms to model the P and S data. The slip model developed based on the teleseismic P waves assuming the location from the CNDSN as a rupture initiation point, including the linear strike orientation (W18°N) of the inferred fault, is displayed in the top Figure 2. The middle panel shows the asperity established from the satellite data, and the bottom panel shows when both surface deformation from the satellite data and teleseismic waveforms were inverted jointly.

The top panel in Figure 3 shows the geo-coded interferogram obtained by combining three separate geo-coded interferograms that resulted from processing satellite data over the entire length of the Kunlun fault. Satellite data came from three tracks, namely 305, 33, and 26. The star shows the epicentral location taken from the CNDSN catalog and is off from the fault that is clearly demarcated in the satellite data. The fault is a steeply dipping fault and its hypocenter should remain almost on the fault track. The bias in the CNDSN location is due to the station distribution as the majority of the CNDSN stations were located in the southwest quadrant of the epicenter.

During the last Seismic Research Review (SRR) meeting, we showed a complex slip model obtained from the combined inversion of the satellite data and teleseismic waveforms that produced a very good fit to all data (bottom panel in Figure 2), but its major feature is similar to the slip model developed based on the satellite data alone. In this presentation, we therefore present results that were further carried out in regards to the sensitivity of the location that is inferred based on our method. Figure 4 (left panel) shows the sensitivity of the teleseismic waveforms for four different hypocenters along the strike of the fault by keeping the depth fixed. Similarly, we also varied the depth of the event, but kept the epicentral location fixed and results are shown in Figure 4 (right panel). For each case, the error estimate is displayed at the upper left corner of each inversion result. Clearly, if we were to compare only the waveforms, it would have been difficult to constrain the location; however, the objective function (Saikia et

al., 2004) used to define the best fit converges to the same location that was obtained by the synergy between the InSAR and seismic methods.

Next, we fixed its hypocenter and used travel times from all Chinese stations (station locations were earlier provided by Dr. Paul G. Richards, Lamont Doherty Observatory) and a local velocity model to estimate the origin time of the event, thus establishing its best location that has the following parameters: origin time 10h02m50.69s, 35.295ºN, 87.5084ºE.

March 5, 2001, (M_w 5.7) Tibet Aftershock

During the 26th SRR meeting, we showed modeling of the teleseismic waveforms for this earthquake indicating that its depth is less than 6 km rather than a depth of 38.9 km reported in the ISC catalog. Regional waveform modeling also suggested a depth consistent with the teleseismic data. Therefore, we hoped to obtain satellite data for this earthquake and use it to relocate the event in conjunction with the seismic data. Although the archive of the satellite database indicated that satellite data were acquired, we could not locate them at EURIMAGE and further study could not be pursued.

January 10, 1998 (M_w 5.7) Northeast China Earthquake

Its surface deformation was also presented in the last SRR meeting. Using the location that was obtained from the surface deformation from the satellite data and depth that was obtained from the seismic waveform modeling, we were able to establish its origin time using travel times collected from 85 CNDSN stations within 30° of the event. Based on this new reliable location, we estimated the SSSCs at all CNDSN stations, which in turn we have used to relocate events that occurred in its vicinity.

North Africa: Events in Algeria and Tunisia

Figure 5 shows locations of four events for which we processed satellite data to find their surface deformation. Of the four events, we were able to find surface deformation for two events, one in Algeria (99/12/12, origin time 17h36m56.24s, latitude 35.32ºN, longitude 1.281ºW, h = 4.4 km, NEIC, Mw 5.6) the other in Tunisia (97/03/20, origin time 18h02m17.98s, latitude 34.0046ºN, longitude 8.24ºE, h = 13.6 km, Mw = 5.0, ISC). Several other events occurred in the same location of the Algerian event. By analyzing both the satellite and seismic data as before, we were able to establish their high quality locations. The relocation parameters for the Algerian event are as follows: origin time 17h36m49.30s, latitude 34.963º, longitude 1.209ºE, and depth 5 km. The Tunisia event has the following parameters: origin time 18h02m14.98s, latitude 34.0623ºN, longitude 8.288ºE. and a depth of 2–4 km. Note that depths are based on both the regional and teleseismic waveform analysis. Figure 6 shows the unwrapped interferogram (bottom panel) for the Algerian event. The surface deformation observed in the interferogram (top panel) is noisy, making it difficult to form the geo-coded interferogram. Nonetheless, it was possible to ascertain the location of the event based on the InSAR interferogram shown in the top panel with a GT5 (ground truth) type of the location uncertainty. As before, we used the relocation of this event to calculate the SSSCs at both regional, far-regional, and teleseismic stations, which were in turn used to locate the other earthquakes in its neighborhood (Table 1). Figure 7 shows the geo-coded interferograms for the Tunisia event, which can be seen as a bull's eye formation of fringe pattern inside each rectangle. For this event, we found two sets of satellite data that could be processed and the event could be observed in both of them.

CONCLUSIONS AND RECOMMENDATAIONS

The overall objective of this three-year project is to concentrate on events in North Africa (Algeria, Libya, Morocco, and Egypt), southwest Asia (Iraq and Iran, including China), and the Korean Peninsula. However, this study is primarily focused on the earthquakes occurring in China because of the availability of travel-time data from the Chinese network stations. This study shows that the travel-time data from the CNDSN have great promise for analyzing both the seismic and satellite data together towards establishing GT locations for some moderate-sized Chinese earthquakes (M_w>5.5).

So far, we have established SSSCs for stations located in China using travel times from their earthquake catalog. Thus, we are successful in relocating many events that have occurred in their neighborhood.

Even though the success in North Africa is only 50% in delineating surface deformation in satellite data, we have established reliable (GT5 type) locations for two critical events, one in Algeria and the other in Tunisia. Both these events allowed us to compute SSSCs for nearby events.

REFERENCES

Ji, C., D. J. Wald, and D. V. Helmberger (2002a), Source description of the 1999 Hector Mine, California earthquake, Part I: wavelet domain inversion theory and resolution analysis, *Bull. Seismol. Soc. Am.* 92: 1192–1207.

Ji, C., D. J. Wald, and D. V. Helmberger (2002b), Source description of the 1999 Hector Mine, California Earthquake, Part II: Complexity of Slip History, *Bull. Seismol. Soc. Am.* 92: 1208–1226.

Ji, C., D. V. Helmberger, D. J. Wald, and K. F. Ma (2003), Slip history and dynamic implications of the 1999 Chi-Chi Taiwan, Earthquake, *J. Geophys. Res.* 108: (B9): 2412. doi:10,1029.2002JB001764.

Peltzer, G., F. Crame, and G. King (1999), Evidence of non-linear elasticity of the crust from the Mw 7.6 Manyi (Tibet) Earthquake, *Science* 286: 272–276.

Saikia, C. K., R. Lohman, G, Ichinose, and M. Simons (2003), Ground truth location using a synergy between InSAR and seismic methods, in *Proceedings of the 25th Seismic Research Review—Nuclear Explosion Monitoring: Building the Knowledge Base*, LA-UR-03-6029, Vol.1, pp. 324–333.

Saikia, C. K, C. Ji, G. A. Ichinose, D. V. Helmerger, A. O. Konca, and M. Simons (2004), Ground truth locations using synergy between remote sensing and seismic methods—application to Chinese earthquakes, in *Proceedings of the 26th Seismic Research Review: Trends in Nuclear Explosion Monitoring*, LA-UR-04-5801,Vol. 1, pp. 328-337.

Tapponier, P. and P. Molnar (1977), Active faulting and tectonics in China, *J. Geophys. Res*. 82: 2905–2930.

Table 1. Relocation Parameters of Earthquakes That Occurred in the Proximity of the Algerian Event. (Relocations are after the SSSCs were applied.)

Date	Origin Time Hr:mn:ss	Latitude (ºN)	Longitude (ºE)	Erx (km)	Ery (km)	RMS (sec)	H (km)
02/12/01	08:38:02.09	35.410	-0.981	35.9	21.2	0.59	-
	08:37:56.80	35.173	-0.783	27.0	16.2	0.37	2.8
00/08/23	00:42:01.19	35.158	-1.300	14.5	8.3	0.40	93
	00:41:54.10	35.081	-1.184	10.3	6.0	0.24	18
00/05/23	12:26:27.73	35.579	-1.442	11.5	6.8	0.39	0.2
	12:26:25.99	35.454	-1.290	12.4	7.1	0.37	2.0
00/01/02	07:05:43.10	35.465	-1.399	89.9		0.82	
	07:05:43.8	35.669	-1.451	9.8		0.47	
00/01/06	11:56:14.93	35.798	-1.734	22.6		0.69	39.8
	11:56:04.00	35.468	-1.403	15.6		0.36	
00/01/27	14:43:27.03	35.328	-1.449	13.2		**0.40**	
	14:43:29.60	35.019	-1.118	19.1		**0.54**	
00/03/18	01:29:07.86	35.434	-1.431	18.5		0.54	1.2
	01:29:03.92	35.317	-1.293	8.6		0.21	1.2
00/07/30	01:05:13.31	35.301	-1.372	10.4		0.67	0.0
	01:05:10.23	34.947	-1.100	6.3		0.34	40.0
99/12/25	21:23:14.04	35.145	-1.326	16.0		**0.38**	
	21:23:08.77	34.935	-1.114	14.8		**0.41**	
99/12/23	00:48:19.41	35.615	-1.415	7.8		**0.46**	0.0
	00:48:07.24	34.993	-0.822	15.3		**0.53**	0.0
99/12/22	18:14:19.76	35.359	-1.426	16.4	9.4	0.52	38.3
	18:14:08.30	34.973	-1.163	15.5	8.6	0.35	1.2
99/12/22	18:32:49.12	35.355	-1.198	12.5		0.75	8.8
	18:32:42.31	35.101	-1.367	7.9		0.49	0.0
97/12/19	15:32:21.98	35.388	-0.871	8.1		0.44	
	15:32:18.54	35.316	-0.736	22.8		0.39	
95/11/21	00:25:10.67	35.522	-0.951	7.6	5.1	0.78	0.0
	00:24:56.86	34.798	-0.253	8.1	11.5	0.29	0.0
95/06/05	09:29:36.57	35.462	-2.478	10.8		0.81	
	09:29:27.45	34.909	-2.345	24.4		0.43	

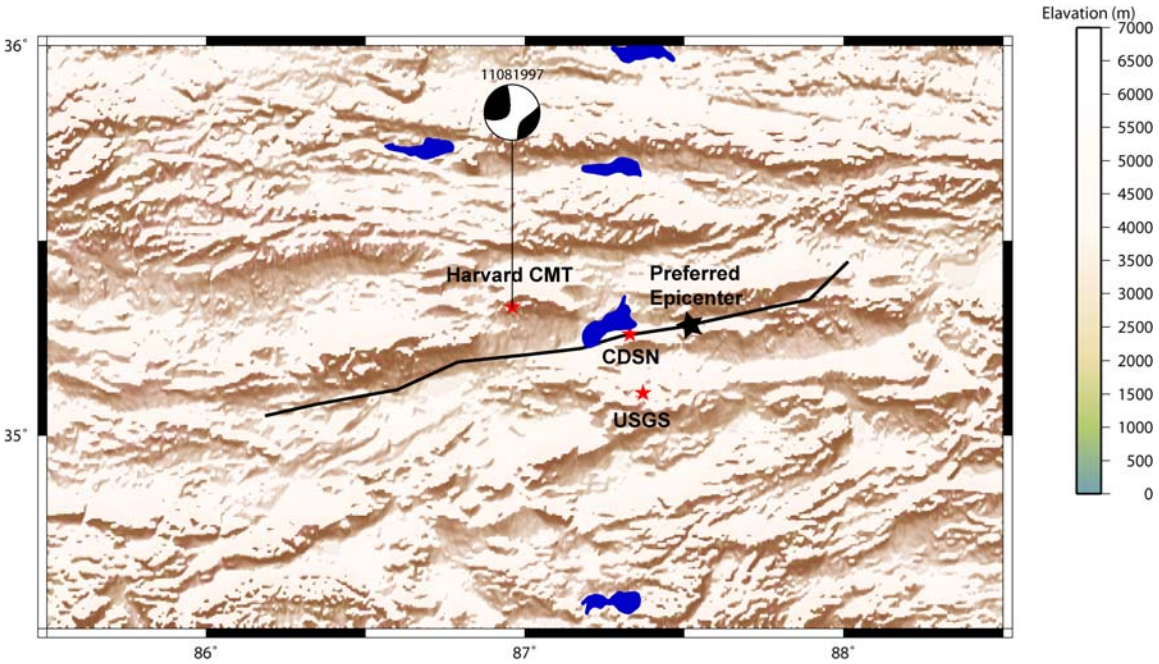

Figure 1. Map with proposed epicenters in red along with our preferred location for the November 8, 1997, Tibet (Manyi) earthquake. The fault breakage is indicated with the heavy dark line.

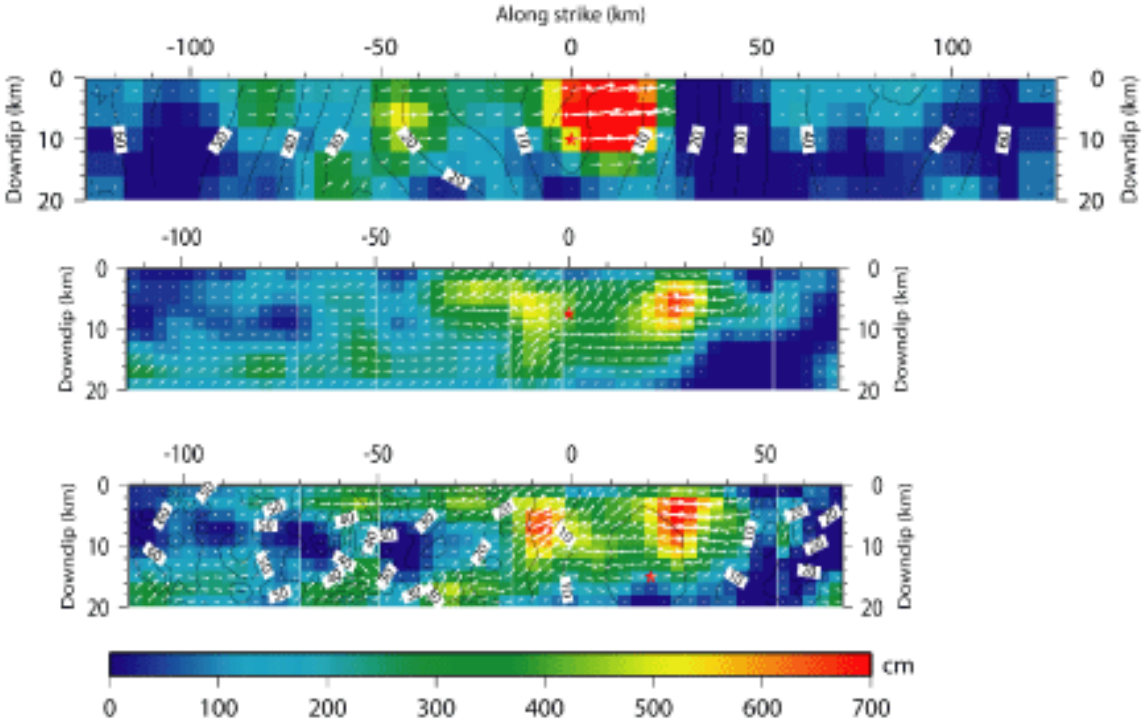

Figure 2. Three panels of slip distributions: top (teleseismic waveforms only), middle (geodetic only, InSAR), and bottom (combined teleseismic and InSAR). Contour lines are included indicating the positions of the rupture front as a function of time after onset. Note that the location of the CDSN epicenter has been shifted 20 km to the right in the bottom panel.

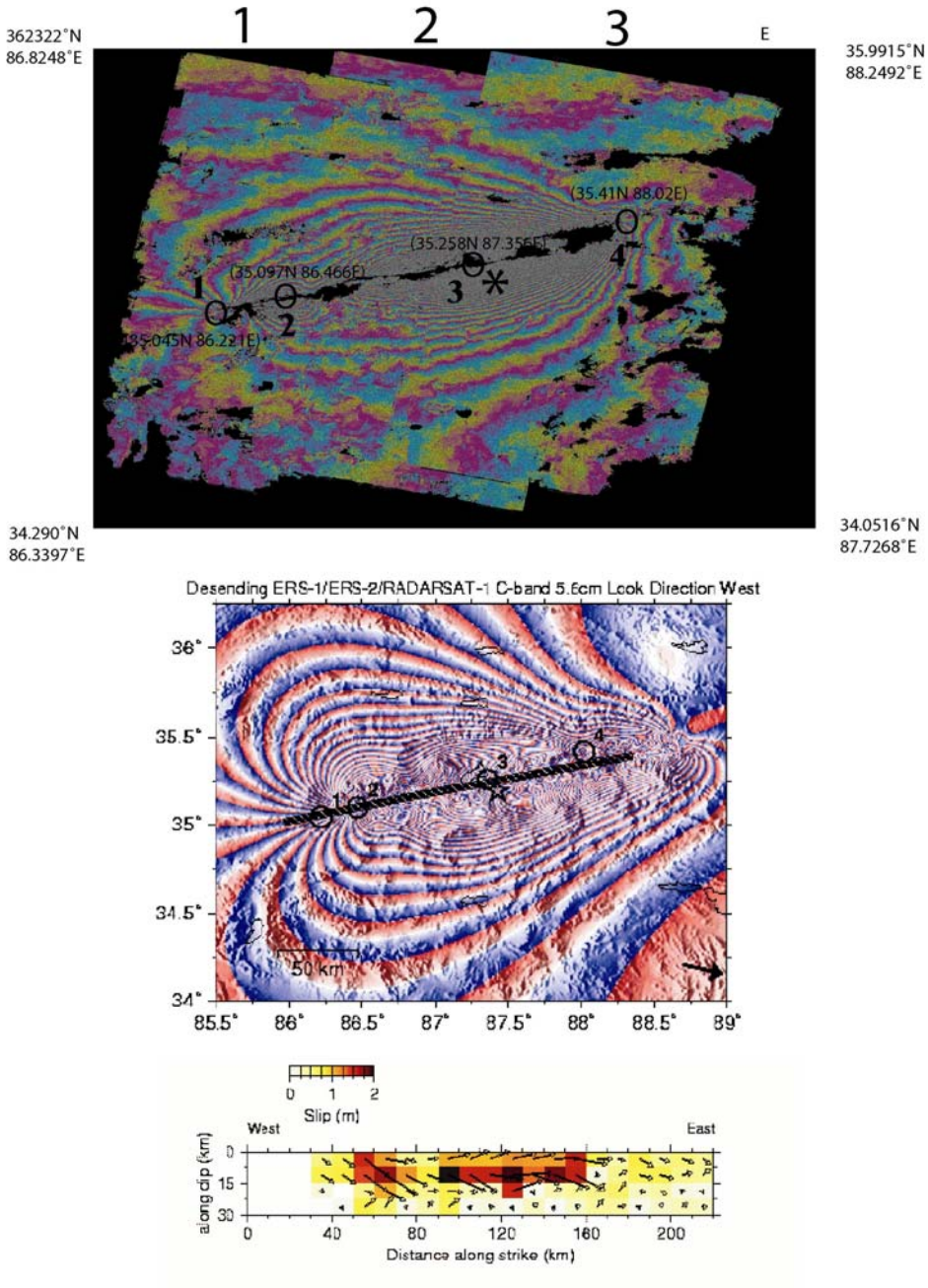

Figure 3. The top panel shows the geo-coded interferograms formed by joining three separate geo-coded interferograms obtained by processing satellite data to cover the entire Kunlun fault. The middle panel shows predicted interferogram using the slip model (bottom panel) obtained by inverting the teleseismic waveform alone. There is an overall match in the fringe pattern match seen in the observation.

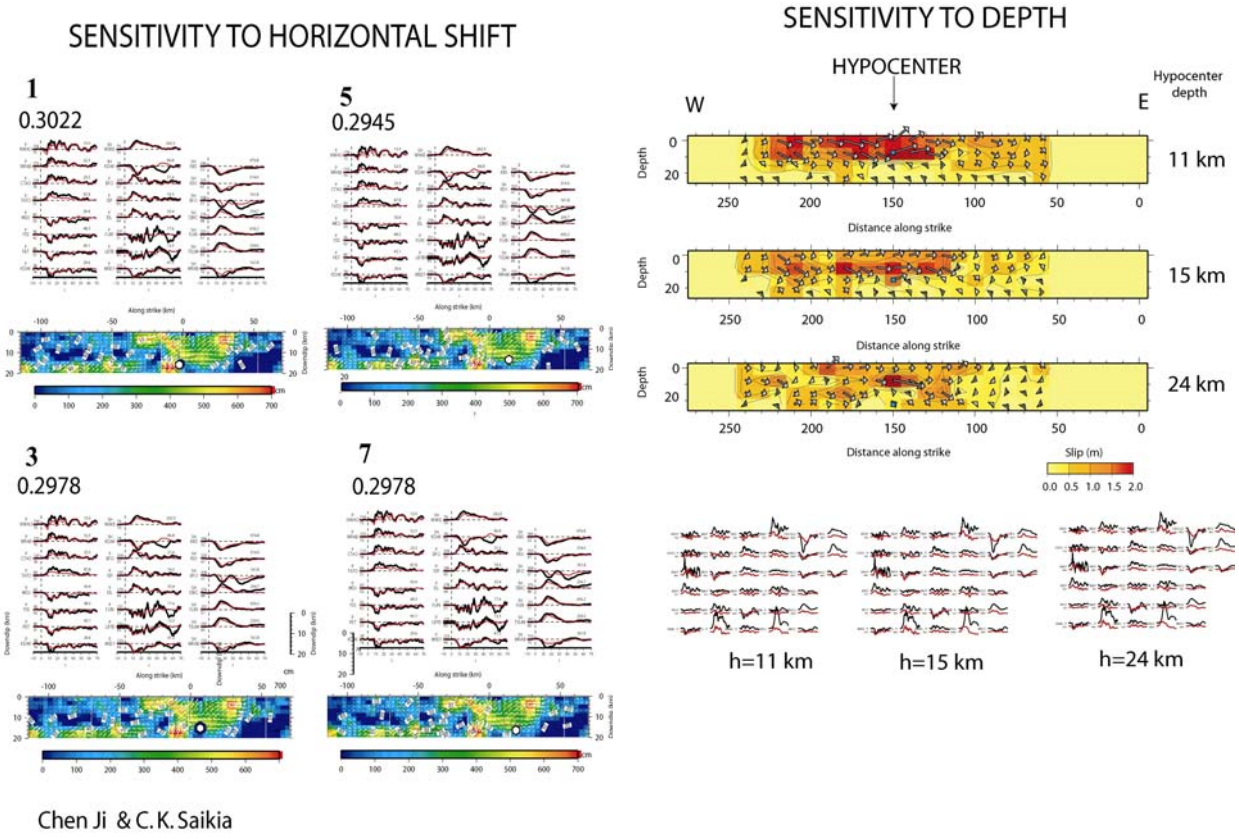

Figure 4. Sensitivity analysis of the teleseismic waveforms to various locations of the hypocenter. The left panel shows the comparison of the observed (black lines) and predicted (red lines) seismograms when the hypocenter was placed at a fixed depth, but at different locations along the strike of the fault. For each case, both InSAR deformation and teleseismic waveforms were jointly inverted. The right panel shows the same for the variation only in depth, but for the teleseismic data. Clearly, teleseismic waveform fit alone cannot distinguish one set of data comparison to the other set of the data comparison. However, the case 5 (left panel) appears to be the global minimum, which is obtained based on the objective function discussed in Saikia et al. (2004).

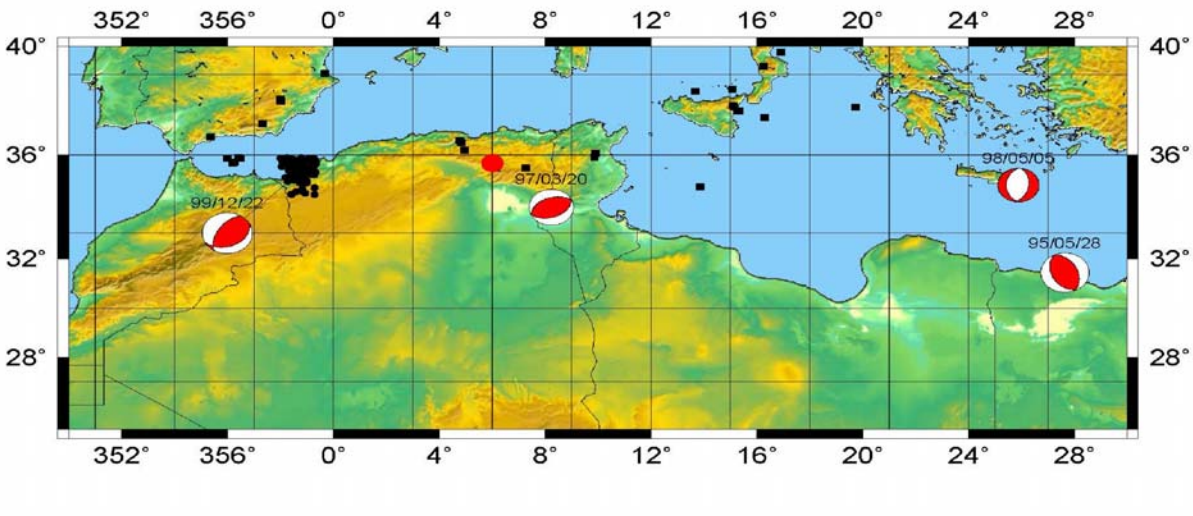

Figure 5. We processed satellite data for events lying within Northern Africa. Of the four events analyzed here, we were able to identify surface deformation in the case of two events. As expected, these events are shallow. These shallow depths were confirmed by modeling both seismic and InSAR data separately.

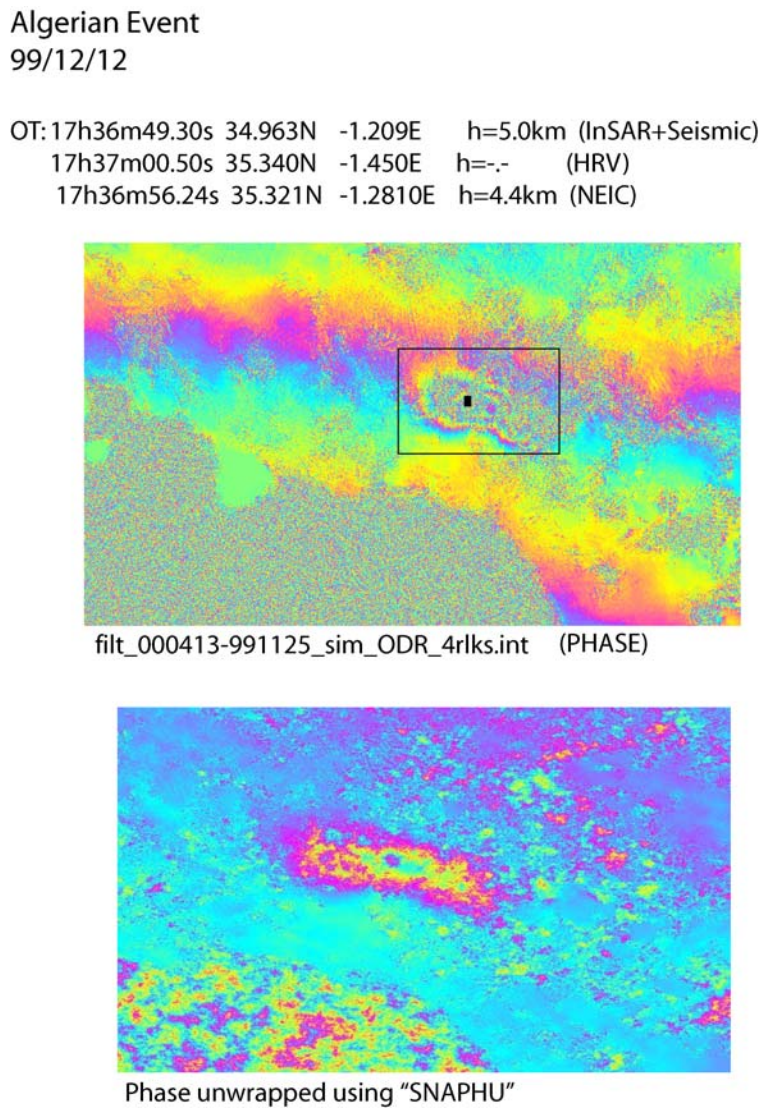

Figure 6. Interferogram processed using the satellite data for the December 12, 1999, Algerian earthquake. It was difficult to unwrap this interferogram by the routine ROI_PAC phase unwrapping schemes. We used a separate code "SNAPHU" to unwrap the phase, which is shown in the bottom panel

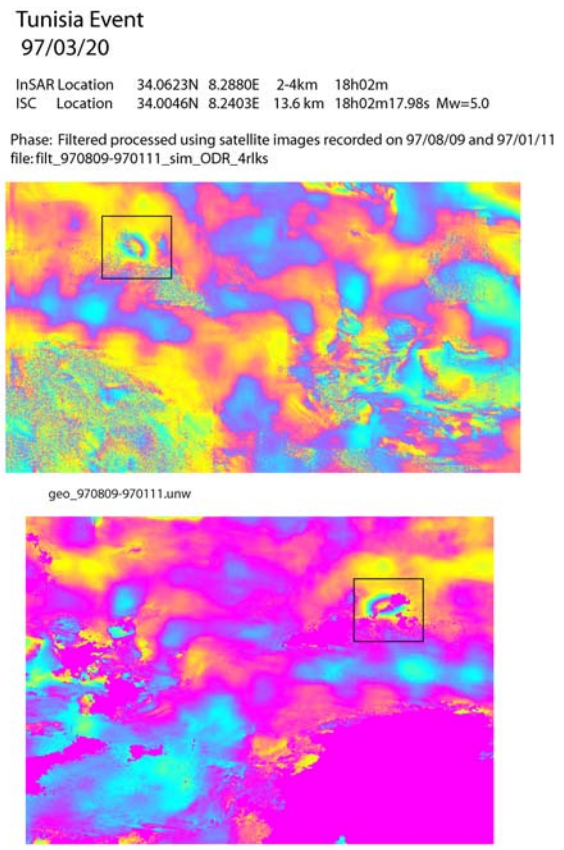

Figure 7. Two geo-coded interferograms for the March 20, 1997, Tunisia event processed using the satellite data acquired from EURIMAGE. The event can be seen in both the interferograms. The DEM was used from the SRTM database.